Stochastic manifestation of chaos

L. E. Reichl, Zhong-Ying Chen, and M. M. Millonas
Center for Statistical Mechanics, University of Texas at Austin, Austin, Texas 78712
(Received 24 July 1989)

We use Floquet theory to study the dynamical properties of a Fokker-Planck equation with time-dependent coefficients describing a nonlinear Brownian rotor driven by a time-periodic angle-dependent external force consisting of two traveling sine waves with amplitudes ϵ_1 and ϵ_2. For the case $\epsilon_2=0$, the Fokker-Planck equation is separable (in the sense that it has two well-defined eigennumbers), and the nearest-neighbor spacing distribution appears to be Poisson random for large ϵ_1. For both $\epsilon_1\neq 0$ and $\epsilon_2\neq 0$, we find evidence of nonlinear resonance and level repulsion in the Floquet spectrum and first-passage time, and the spectrum exhibits level repulsion and universal random matrix-type behavior. The long-time state is quasiperiodic in time and angle and is affected by an increasing number of modes of the system as the external field amplitude is increased.

I. INTRODUCTION

The transition to chaos in nonlinear conservative classical-mechanical systems has been found to manifest itself in the corresponding quantum systems as a transition in the energy (or quasienergy for periodically driven systems) spectral statistics as a parameter of the system is varied.[1-4] For bound quantum systems with discrete spectrum this transition is not accompanied by the onset of chaos (sensitive dependence on initial conditions) as it is in the corresponding classical system. It does, however, appear to be accompanied by a loss of the possibility to assign a complete set of quantum numbers to some of the eigenstates and therefore a loss of information about the dynamics of the system. For systems which have a full set of quantum numbers the nearest-neighbor spacings between spectral lines is random and satisfies a Poisson distribution. As the transition to chaos occurs, the nearest-neighbor spacing distribution changes from Poisson to a random matrix-type distribution characterized by resonance and level repulsion. This transition is also accompanied by extension of the energy (or quasienergy) eigenstates of the system and can lead to a change in the dynamical behavior of the system.

This transition in the spectral spacing statistics has also been observed by Grobe, Haake, and Sommers[5] in weakly dissipative quantum systems (the quantum delta kicked rotor with dissipation) whose classical frictionless counterpart undergoes a transition to chaos. The system studied by Grobe, Haake, and Sommers has a complex spectrum and also exhibits a transition in its nearest-neighbor spacing statistics from Poisson to random matrix type. However, since the spectrum is complex, the Poisson distribution is that of nearest neighbors in a plane rather than on a line, and the random matrix nearest-neighbor spacing distribution corresponds to that of an asymmetric matrix rather than that of a Hermitian matrix as is the case for nondissipative quantum systems.

In this paper, we consider the case of a driven rotor undergoing Brownian motion in a highly viscous fluid. The frictionless classical-mechanical and quantum-mechanical versions of this system undergo a transition to chaos (in the quantum case there is a transition in the spectral statistics) as the amplitude of the driving force is increased. In the limit of large viscosity we can write a Fokker-Planck equation (the Smoluchowsky equation) with periodic time-dependent coefficients for the probability density $P(\theta,t)$ to find the rotor in the interval θ to $\theta+d\theta$ at time t. We can use Floquet theory to reduce the solution of the Fokker-Planck equation to an eigenvalue problem. The matrix that determines the time evolution of the Fokker-Planck equation is asymmetric and has complex eigenvalues.

We shall consider the driven Brownian rotor for two different cases. In one case the Fokker-Planck equation is separable and in the second it is not. We shall show that in the first case, the Floquet spectrum is Poissonian for large driving field amplitude, while for the second case we observe nonlinear resonance and level repulsion in the Floquet spectrum for large driving field amplitude. We begin in Sec. II by describing the Brownian rotor model and we explicitly write the difference equations of the mode amplitudes for the two cases considered. In Sec. III, we derive explicit expressions for the Floquet matrices which determine the time evolution and in Sec. IV we describe the general properties of the spectrum in the two cases. In Sec. V, we plot the first-passage time as a function of both external field frequency and amplitude. We see evidence in the first-passage time of resonance phenomena and the transition in the spectrum. In Sec. VI, we plot histograms which indicate quite different spectral spacing distributions for the two cases. For the separable case we find Poisson-like behavior and for the nonseparable case we find a transition to random matrix-like behavior. In Sec. VII, we study the behavior of one of the Floquet eigenvectors which govern the long-time behavior of the system as a function of driving field amplitude. We find that, although the eigenvalues that govern the long-time behavior do not depend on driving field amplitude, the eigenvectors do. For this system the long-time states are quasiperiodic in time and angle. For low external driving field amplitude, they contain only a

few modes, but for larger external driving field amplitude, they contain many Fourier components. Finally, in Sec. VIII, we make some concluding remarks.

II. MODEL

We will consider a Brownian rotor that consists of a spherical mass m with radius a attached to a massless rigid rod of length L and zero radius immersed in a fluid with shear viscosity η. The motion of the rotor is constrained to lie in the x-y plane. The Langevin equation describing the Brownian motion of this rotor is

$$I\frac{d\Omega}{d\tau}=-\gamma\Omega+\mathcal{T}_{\rm rand}(\tau)+\mathcal{T}_{\rm ex}(\theta,\tau)\ , \tag{2.1}$$

where Ω $(=\dot{\theta})$ and θ are the angular velocity and angle, respectively, of the rotor at time τ, $I=mL^2$ is the moment of inertia, $\mathcal{T}_{\rm rand}(\tau)$ is the δ-function-correlated Langevin torque due to the fluid, $\gamma=6\pi a\eta$ is the Stokes friction, and $\mathcal{T}_{\rm ex}(\theta,\tau)$ is the torque due to any externally applied fields. The random torque has the property that the correlation function

$$\langle\mathcal{T}_{\rm rand}(\tau)\mathcal{T}_{\rm rand}(\tau')\rangle=q\delta(\tau-\tau')\ ,$$

where $q=2\gamma k_BT$, T is the temperature, and k_B is Boltzmann's constant. The Fokker-Planck equation for the probability density $\mathcal{P}(\Omega,\theta,t)$ of the Brownian rotor can then be written

$$\frac{\partial\mathcal{P}}{\partial\tau}=-\frac{\partial}{\partial\theta}(\Omega\mathcal{P})+\frac{\partial}{\partial\Omega}\left[\left[\frac{\gamma\Omega}{I}-\frac{\mathcal{T}_{\rm ex}}{I}\right]\mathcal{P}\right]+D\frac{\partial^2\mathcal{P}}{\partial\Omega^2}\ , \tag{2.2}$$

where $D=k_BT/\gamma$.

In the present paper, we shall consider this system in the limit of a very large Stokes friction, so that the angular velocity of the rotor relaxes to equilibrium on a time scale that is short compared to the time scales associated with the external torque $\mathcal{T}_{\rm ex}(\theta,\tau)$. Then inertial effects may be neglected in Eq. (2.1) and the Langevin equation becomes

$$\gamma\Omega=\mathcal{T}_{\rm rand}(\tau)+\mathcal{T}_{\rm ex}(\theta,\tau)\ . \tag{2.3}$$

In this limit, the equation of motion for the reduced distribution $P(\theta,\tau)$ is given by the Smoluchowski equation[6]

$$\frac{\partial P(\theta,\tau)}{\partial\tau}=-\frac{1}{\gamma}\frac{\partial}{\partial\theta}[\mathcal{T}_{\rm ex}(\theta,t)P]+D\frac{\partial^2P}{\partial\theta^2}\ . \tag{2.4}$$

We shall study the behavior of the Smoluchowski equation for the case of an applied torque of the form

$$\mathcal{T}_{\rm ex}(\theta,\tau)=\mathcal{T}_1\sin(\theta-\omega\tau)+\mathcal{T}_2\sin(\theta+\omega\tau)\ . \tag{2.5}$$

It is convenient to change to dimensionless parameters. Let $t=D\tau$, $\omega_0=\omega/D$, and $\epsilon_i=\mathcal{T}_i/\gamma D$. Then we obtain

$$\frac{\partial P(\theta,\tau)}{\partial t}=-\frac{\partial}{\partial\theta}[f(\theta,t)P]+\frac{\partial^2P}{\partial\theta^2}\ , \tag{2.6}$$

where $f(\theta,t)=\epsilon_1\sin(\theta-\omega_0\tau)+\epsilon_2\sin(\theta+\omega_0\tau)$. Thus the behavior of the system is entirely determined in terms of three dimensionless parameters, the amplitudes ϵ_i, and frequency ω_0. The probability density $P(\theta,t)$ satisfies the boundary condition $P(\theta,t)=P(\theta+2\pi,t)$. Thus we can expand $P(\theta,t)$ in a Fourier series in the angle θ. We will consider the behavior of this system for two different cases.

Case I: $(\epsilon_1=\epsilon,\epsilon_2=0)$. In this case the Smoluchowski equation is separable and can be reduced to that of a simple pendulum in a viscous medium. It is interesting to note that in the absence of friction and noise the mechanical system is integrable. In order to obtain the Floquet spectrum for this system, we must first write the Smoluchowski equation in terms of its Fourier components. For Case I, we expand $P(\theta,t)$ in the Fourier series

$$P(\theta,t)=\sum_{n=-\infty}^{\infty}c_n(t)e^{in\theta}\ . \tag{2.7}$$

The equation of motion for the coefficients $c_n(t)$ is then given by

$$\frac{\partial c_m}{\partial t}=-m^2c_m-\frac{m}{2}[\epsilon(c_{m-1}e^{-i\omega_0t}-c_{m+1}e^{i\omega_0t})]. \tag{2.8}$$

As we shall show, for this case the Fokker-Planck equation is separable.

Case II: $(\epsilon_1=\epsilon_2=\epsilon)$. In this case the Smoluchowski equation appears not to be separable and its spectrum exhibits evidence of resonance and level repulsion. In the absence of viscosity and noise, this mechanical system exhibits a transition to chaos.[4,7] For case II, we expand $P(\theta,t)$ in the Fourier series

$$P(\theta,t)=a_0(t)\phi_0^{(e)}+\sum_{n=1}^{\infty}[a_n(t)\phi_n^{(e)}(\theta)+b_n(t)\phi_n^{(0)}(\theta)]\ . \tag{2.9}$$

If we introduce the scalar product

$$\langle\phi_n^{(i)},\phi_{n'}^{(j)}\rangle=\int_0^{\infty}\frac{\phi_n^{(i)}(\theta)\phi_{n'}^{(j)}(\theta)}{\phi_0(\theta)}d\theta=\delta_{n,n'}\delta_{i,j}\ , \tag{2.10}$$

then $\phi_0(\theta)=1/2\pi$, the even mode $\phi_n^{(e)}(\theta)=(1/\sqrt{2}\pi)\cos(n\theta)$, and the odd mode $\phi_n^{(o)}(\theta)=(1/\sqrt{2}\pi)\sin(n\theta)$. Using these expressions, we find that the equations for the coefficients $a_m(t)$ and $b_m(t)$ decouple. We then obtain the following equation for the coefficients $a_m(t)$:

$$\frac{\partial a_m(t)}{\partial t}=-m^2a_m(t)-\epsilon\sin(\omega_0t)\sum_{n=0}^{\infty}V_{m,n}a_n(t)\ , \tag{2.11}$$

where $V_{0,m}=0$ for $0\le m\le\infty$, $V_{1,0}=1/\sqrt{2}$, and $V_{m,n}=(m/2)(\delta_{n,m+1}-\delta_{n,m-1})$ for $1\le m\le\infty$. We shall call this case IIa. Similarly, the equations for the coefficients $b_n(t)$ can be written

$$\frac{\partial b_m(t)}{\partial t}=-m^2b_m(t)-\epsilon\sin(\omega_0t)\sum_{n=1}^{\infty}V_{m,n}b_n(t)\ , \tag{2.12}$$

for $1\le m$ and $n\le\infty$. We call this case IIb. Thus, for case II the even and odd modes $\phi_n^{(e)}(\theta)$ and $\phi_n^{(o)}(\theta)$ are completely uncoupled. Furthermore, the coefficient a_0 is determined completely by the initial conditions and can-

not change in time.

We have used different Fourier expansions for case I and case II to facilitate the decomposition of the Floquet matrix (to be derived in the next section) into block diagonal form. In the next section, we show how to use the Floquet theory to study the time evolution of this dynamically driven stochastic system.

III. FLOQUET THEORY

Let us write Eqs. (2.8), (2.11), and (2.12) in the abstract form

$$\frac{\partial\langle m|\mathcal{C}_{(\alpha)}(t)\rangle}{\partial t}=\sum_n\langle m|\mathcal{V}_{(\alpha)}(t)|n\rangle\langle n|\mathcal{C}_{(\alpha)}(t)\rangle\ , \tag{3.1}$$

with $\alpha=a$, b, and c, respectively. Thus Eq. (3.1) reduces to Eqs. (2.8), (2.11), and (2.12) when $c_n(t)=\langle n|\mathcal{C}_{(c)}(t)\rangle$, $a_n(t)=\langle n|\mathcal{C}_{(a)}(t)\rangle$, and $b_n(t)=\langle n|\mathcal{C}_{(b)}(t)\rangle$, respectively. The matrices $\langle m|\mathcal{V}_{(\alpha)}(t)|n\rangle$, for $\alpha=a$, b, and c, are given in the Appendix.

Since $\mathcal{V}_{(\alpha)}(t)$ is periodic in time, $\mathcal{V}_{(\alpha)}(t)=\mathcal{V}_{(\alpha)}(t+T)$ where $T=2\pi/\omega_0$. Thus we can assume that Eq. (3.1) has Floquet-type solutions $\langle n|\Psi_i^{(\alpha)}(t)\rangle$ (where $i=1,\ldots,\infty$) such that

$$\langle n|\Psi_i^{(\alpha)}(t+T)\rangle=e^{\Lambda_i^{(\alpha)}T}\langle n|\Pi_i^{(\alpha)}(t)\rangle\ , \tag{3.2}$$

and

$$\langle n|\Psi_i^{(\alpha)}(t)\rangle=e^{\Lambda_i^{(\alpha)}t}\langle n|\Pi_i^{(\alpha)}(t)\rangle\ , \tag{3.3}$$

In Eq. (3.3), $\langle n|\Pi_i^{(\alpha)}(t)\rangle$ is a periodic function of time, $\langle n|\Pi_i^{(\alpha)}(t+T)\rangle=\langle n|\Pi_i^{(\alpha)}(t)\rangle$. Since $\langle n|\Pi_i^{(\alpha)}(t)\rangle$ is periodic in time, we can expand it in a Fourier series. Then Eq. (3.13) takes the form

$$\langle n|\Psi_i^{(\alpha)}(t)\rangle=\sum_{q=-\infty}^{\infty}\langle n,q|\pi_i^{(\alpha)}\rangle e^{-iq\omega_0 t}e^{\Lambda_i^{(\alpha)}t} \tag{3.4}$$

where $\langle n,q|\pi_i^{(\alpha)}\rangle$ is the Fourier amplitude in the Fourier transform of $\langle n|\Pi_i^{(\alpha)}(t)\rangle$.

If we substitute Eq. (3.4) into (3.1), we obtain the following matrix equation for the Fourier coefficients $\langle n,q|\pi_i^{(\alpha)}\rangle$ and Floquet parameters $\Lambda_i^{(\alpha)}$:

$$\Lambda_i^{(\alpha)}\langle m,q|\pi_i^{(\alpha)}\rangle=\sum_n\sum_{q'=-\infty}^{\infty}\langle m,q|\mathcal{W}_{(\alpha)}|n,q'\rangle\langle n,q'|\pi_i\rangle\ , \tag{3.5}$$

where

$$\langle m,q|\mathcal{W}_{(\alpha)}|n,q'\rangle=\frac{1}{2\pi}\int_{-\infty}^{\infty}dt\,e^{i(q-q')t}\langle m|\mathcal{V}_{(\alpha)}(t)|n\rangle\ , \tag{3.6}$$

and the range of the integers m and n depends on whether we consider case I or case II. The quantity $\mathcal{W}_{(\alpha)}$ is the Floquet transition operator for this stochastic process. It is the stochastic analog of the quasienergy Hamiltonian in driven quantum systems.[8] Expressions for the Floquet transition matrices $\langle m,q|\mathcal{W}_{(\alpha)}|n,q'\rangle$ for the cases $\alpha=a$, b, and c, are given in the Appendix.

Thus we have reduced the solution of the Smoluchowski equation to the solution of the eigenvalue problem

$$\mathcal{W}_{(\alpha)}|\pi_i^{(\alpha)}\rangle=\Lambda_i^{(\alpha)}|\pi_i^{(\alpha)}\rangle\ . \tag{3.7}$$

The Floquet transition matrix $\langle m,q|\mathcal{W}_{(\alpha)}|n,q'\rangle$ is infinite dimensional, complex, and not self-adjoint under Hermitian conjugation. Thus its eigenvalues may be complex and its orthonormal right and left eigenvectors $|\pi_i^{(\alpha)}\rangle$ and $\langle\pi_i^{(\alpha)}|$, respectively, will not be the same. The vector $|\pi_i^{(\alpha)}\rangle$ is the right eigenvector with eigenvalue $\Lambda_i^{(\alpha)}$. We obtain the left eigenvector from the equation $\langle\pi_i^{(\alpha)}|\mathcal{W}_{(\alpha)}=\langle\pi_i^{(\alpha)}|\Lambda_i^{(\alpha)}$. Thus the coefficients $\langle n|\mathcal{C}_{(\alpha)}(t)\rangle$ may be expanded in terms of Floquet states as

$$\langle n|\mathcal{C}_{(\alpha)}(t)\rangle=\sum_{i=1}^{\infty}\sum_{q=-\infty}^{\infty}A_i^{(\alpha)}e^{\Lambda_i^{(\alpha)}t}\langle n,q|\pi_i^{(\alpha)}\rangle e^{iq\omega_0 t}\ , \tag{3.8}$$

where $A_i^{(\alpha)}$ is determined from the initial conditions on $\langle n|\mathcal{C}_{(\alpha)}(0)\rangle$. It is clear from Eq. (3.5) and (A5) that in the limit $\epsilon_i\to 0$, $\Lambda_i^{(\alpha)}\to\Lambda_i^0=-m^2+iq\omega_0$. Thus, for small coupling, the Floquet spectrum is indexed by two "eigen-numbers" m and q, which characterize the unperturbed rotor and the degree of excitation of the external field, respectively. For small ϵ_i, the external field, which is harmonic, adds a strong rigidity to the imaginary part of the spectrum. However, as the coupling increases this rigidity relaxes somewhat.

We can now write the spectral decomposition of the probability $P(\theta,t)$ in terms of Floquet states. For case I, we find

$$P(\theta,t)=\sum_{n=-\infty}^{\infty}\sum_{q=-\infty}^{\infty}\sum_{i=1}^{\infty}A_i^{(c)}e^{\Lambda_i^{(c)}t}\langle n,q|\pi_i^{(c)}\rangle\times e^{iq\omega_0 t}e^{in\theta}\ . \tag{3.9}$$

For case II, we find

$$P(\theta,t)=\sum_{q=-\infty}^{\infty}\sum_{i=1}^{\infty}e^{iq\omega_0 t}\left[A_i^{(a)}e^{\Lambda_i^{(a)}t}\langle 0,q|\pi_i^{(a)}\rangle\phi_0^{(e)}+\sum_{n=1}^{\infty}\left[A_i^{(a)}e^{\Lambda_i^{(a)}t}\langle n,q|\pi_i^{(a)}\rangle\phi_n^{(e)}+A_i^{(b)}e^{\Lambda_i^{(b)}t}\langle n,q|\pi_i^{(b)}\rangle\phi_n^{(o)}\right]\right]\ . \tag{3.10}$$

We shall discuss the nature of these solutions in the following sections.

IV. FLOQUET SPECTRUM

The Floquet matrices for cases I and II have quite different structure and spectral properties and therefore it is useful to discuss their properties separately.

A. Floquet spectrum—case I

The Floquet matrix for case I ($\epsilon_1\neq 0,\epsilon_2=0$) can be written in block diagonal form with an infinite number of infinite-dimensional blocks along its diagonal. We label the different blocks by the integer index β where

$-\infty \leq \beta \leq \infty$. The βth block only connects those states $|m,q\rangle$ whose eigen-numbers satisfy the condition $m+q=\beta$. Thus the spectrum Λ_i for the case ($\epsilon_1 \neq 0, \epsilon_2 = 0$) is a mixed sequence. That is, it is the superposition of an infinite number of pure sequences, one pure sequence coming from each block. In Fig. 1, we show the Floquet spectrum for the block $\beta=0$ taken from the full Floquet matrix with $|m| \leq 23$ and $|q| \leq 23$ and $\omega=1.0$ and $\epsilon=9.0$ and 18.0. For the smaller value of ϵ the spectrum forms a line in the complex plane, while for the larger value of ϵ it appears to break into two lines. The complete spectrum for this 529×529 Floquet matrix is shown in Fig. 2 for the case $\omega=1.0$ and $\epsilon=18.0$. It is the superposition 45 such blocks of sizes varying from 1×1 to 46×46. The Fokker-Planck equation for this case is separable because even for strong coupling there are two well-defined eigen-numbers which label the eigenvalues $\Lambda_i^{(c)}$. One labels the block from which $\Lambda_i^{(c)}$ comes, and the other labels its position in the sequence of eigenvalues coming from that block.

B. Floquet spectrum—case II

For case II ($\epsilon_1 \neq 0, \epsilon_2 \neq 0$), there is no such infinite decomposition of the spectrum. There are two symmetries which allow us to break the Floquet matrix into block diagonal form with four blocks. We have found that the equations of motion for $a_n(t)$ and $b_n(t)$ completely decouple due to the fact that $\mathcal{T}_{ex}(\theta,\tau) = -\mathcal{T}_{ex}(-\theta,\tau)$, yielding a two block Floquet matrix. Each of these two blocks, which we call sine and cosine blocks, further decomposes into two blocks, one in which the states with $n+q$ odd are coupled and the other in which the states with $n+q$ even are coupled. All information about the long-time behavior is contained in the cosine block.

The Floquet eigenvalues $\Lambda_i^{(a)}$ and $\Lambda_i^{(b)}$ can be found by computing eigenvalues of the matrices $\langle m,q|\mathcal{W}_{(a)}|n,q'\rangle$ and $\langle m,q|\mathcal{W}_{(b)}|n,q'\rangle$, respectively. The matrix $\langle m,q|\mathcal{W}_{(a)}|n,q'\rangle (m,n \geq 0; -\infty \leq q,q' \leq \infty)$ has complex eigenvalues. Some of these eigenvalues have zero real parts and determine the long-time behavior of the probability. The remaining eigenvalues have negative real parts and influence the behavior of the system for shorter times and describe contributions which eventually decay to zero. The eigenvalues of the matrix, $\langle m,q|\mathcal{W}_{(b)}|n,q'\rangle (m,n \geq 1; -\infty \leq q,q' \leq \infty)$ all have negative real parts and therefore only give contributions to the time dependence which eventually decay to zero. The matrices $\langle m,q|\mathcal{W}_{(a)}|n,q'\rangle$ and $\langle m,q|\mathcal{W}_{(b)}|n,q'\rangle$ each decompose into two independent submatrices. On one submatrix, the states for which the combination $m+q$ is odd are coupled and in the other the states for which $m+q$ is even are coupled. Thus each of the two matrices $\langle m,q|\mathcal{W}_{(a)}|n,q'\rangle$ and $\langle m,q|\mathcal{W}_{(b)}|n,q'\rangle$ gives rise to two independent sequences of eigenvalues.

As we noted above, the matrix $\langle m,q|\mathcal{W}_{(a)}|n,q'\rangle$ con-

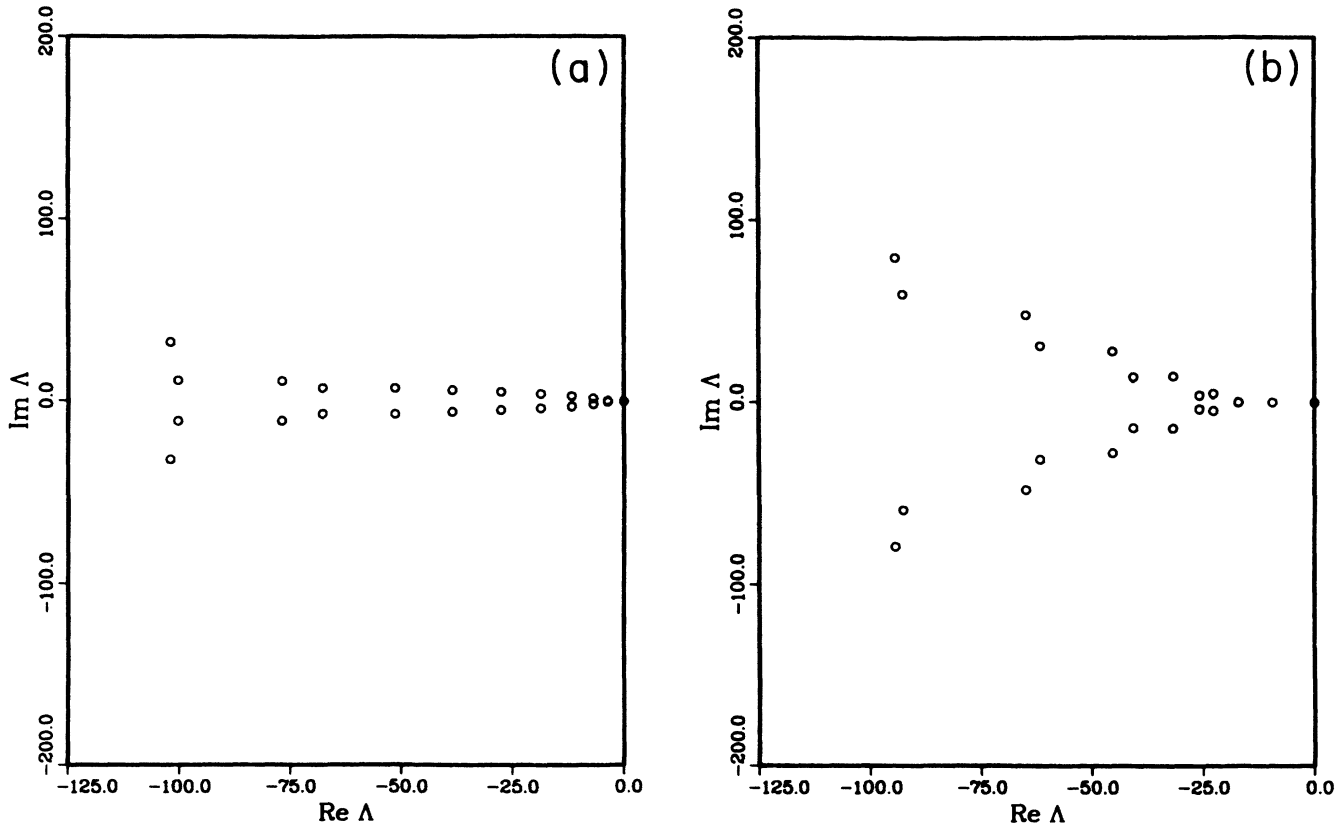

FIG. 1. Eigenvalues for the block $\beta=n+q=0$. The matrix contains 23 eigenvalues and the eigenvalues exhibit a line distribution rather than being randomly scattered in a plane. (a) $\omega_0=1.0$, $\epsilon_1=9.0$, and $\epsilon_2=0$. (b) $\omega_0=1.0$, $\epsilon_1=18.0$, and $\epsilon_2=0$.

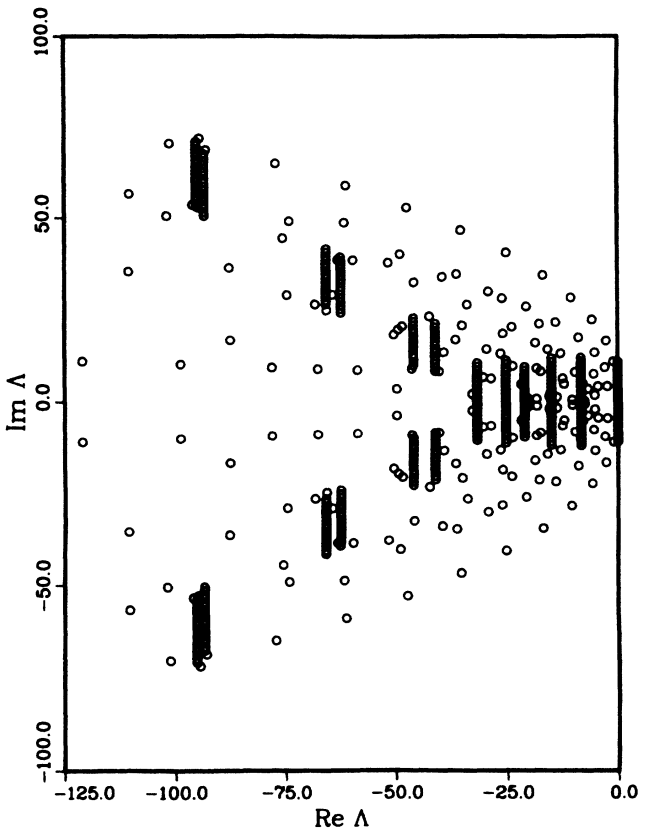

FIG. 2. Floquet spectrum for case I for $\omega_0=1.0$, $\epsilon_1=18.0$, and $\epsilon_2=0$. The spectrum is a superposition of 45 blocks of various sizes ranging from 1×1 to 23×23.

tains information about both the long-time behavior and intermediate-time dependence of the probability density $P(\theta,t)$. It is interesting that the structure of $\langle m,q|\mathcal{W}_{(a)}|n,q'\rangle$ is such that the eigenvalues $\Lambda^{(a)}_{(0,q)}(\epsilon)=iq\omega_0$ regardless of the value of ϵ. However, the eigenstates of $\langle m,q|\mathcal{W}_{(a)}|n,q'\rangle$ with eigenvalues $\Lambda^{(a)}_{(0,q)}(\epsilon)=iq\omega_0$ do depend on the value of ϵ. We say more about this in Sec. VII.

In Ref. 9 we found that the real part of the lowest Floquet eigenvalue undergoes an abrupt transition at $\omega_0\approx\epsilon$. The same behavior is observed in this system. This is apparently the result of the fact that the dominant contribution from the external driving field in the square well system (the system studied in Ref. 9) is of the form $\cos(\theta-\omega_0 t)$ as it is for the system studied here.

For case II, we have observed evidence of nonlinear resonance and level repulsion. In Fig. 3, we show the Floquet spectrum Λ_i for $\omega_0=10.0$ and for a range of values of ϵ ($\epsilon=10.0, 10.2, 10.5, 12.0, 12.5, 13.0$) which show movement of a nonlinear resonance down the real Λ axis. For these values of ϵ the spectrum still contains a large degree of rigidity as is evident in the figure. We see that with increasing values of ϵ, the real part of the spectrum (the nonlinear part) appears to resonant and repel. This resonance region runs down the real axis until it reaches the lowest excited state and shifts the real part to larger negative values. (This is the origin of the shift in the real part of the Floquet eigenvalue observed in Ref. 8.) This shifting of eigenvalues causes a fairly abrupt drop in the first-passage time for this system as we shall show in the next section.

It is also of interest to look at the spectrum for different values of ω_0 and ϵ. In Fig. 4, we show the location of eigenvalues for $\omega_0=1.0$ and for $\epsilon=1.0$ and 9.0. To obtain Fig. 4, we have diagonalized a 390×390 submatrix for case IIa ($n\leq20$) and $q\leq20$). The spectrum for $\epsilon=1.0$ [Fig. 4(a)] shows the rigidity and regularity typical of the Floquet spectrum for small ϵ (small means $\epsilon<\omega_0$). In this figure resonance is occurring, but is not obvious from the figure. In Fig. 4(b), we see that where $\epsilon\gg\omega_0$, the Floquet eigenvalues with a small real part have become quite chaotic in appearance.

V. FIRST-PASSAGE TIME

The first-passage time is the average limit it takes for a Brownian particle to reach some point on its path for the first time. It can provide a means of quantifying qualitative changes in the spectral properties provided the spectrum is unchanged in setting up the first-passage-time equations. To obtain an expression for the first-passage time let us assume that the Brownian rotor is located at $\theta=\pi/2$ at time $t=0$ and that absorbing barriers are located at $\theta=0$ and at $\theta=\pi$. With this initial condition, $P(\theta,t)$ is a conditional probability $P(\theta,t)\equiv P(\theta,t|\pi/2,0)$, where $P(\theta,0|\pi/2,0)=\delta(\theta-\pi/2)$, and Eq. (2.6) may then be thought to describe the evolution of this conditional probability. With these absorbing barriers in place the conditional probability satisfies the boundary conditions $P(0,t|\pi/2,0)=P(\pi,t|\pi/2,0)=0$. Let S denote the interval $0\leq\theta\leq\pi$. Then the probability to find the rotor in S at time t is

$$P_S\left[\frac{\pi}{2},t\right]=\int_0^{\pi}P\left[\theta,t|\frac{\pi}{2},0\right]d\theta\ . \tag{5.1}$$

The first-passage time is the average time $\langle t\rangle$ that it takes the rotor to reach the absorbing boundary for the first time. Let $F(\pi/2,t)dt$ denote the probability that the rotor reaches the absorbing wall in the time interval $t\rightarrow t+dt$. Then

$$P_S\left[\frac{\pi}{2},t\right]=F\left[\frac{\pi}{2},t\right]dt+P_S\left[\frac{\pi}{2},t+dt\right]\ . \tag{5.2}$$

Thus

$$F\left[\frac{\pi}{2},t\right]=-\frac{dP_S(\pi/2,t)}{dt}\ , \tag{5.3}$$

and the nth moment of the first-passage time is given by

$$\langle t^n\rangle=\int_0^{\infty}t^nF\left[\frac{\pi}{2},t\right]dt=n\int_0^{\infty}t^{n-1}P_S\left[\frac{\pi}{2},t\right]dt\ , \tag{5.4}$$

where we have integrated by parts to obtain the last term.

Since the probability $P(\theta,t|\pi/2,0)$ must be zero at the walls, we can expand its angle dependence in a Fourier sine series. Thus

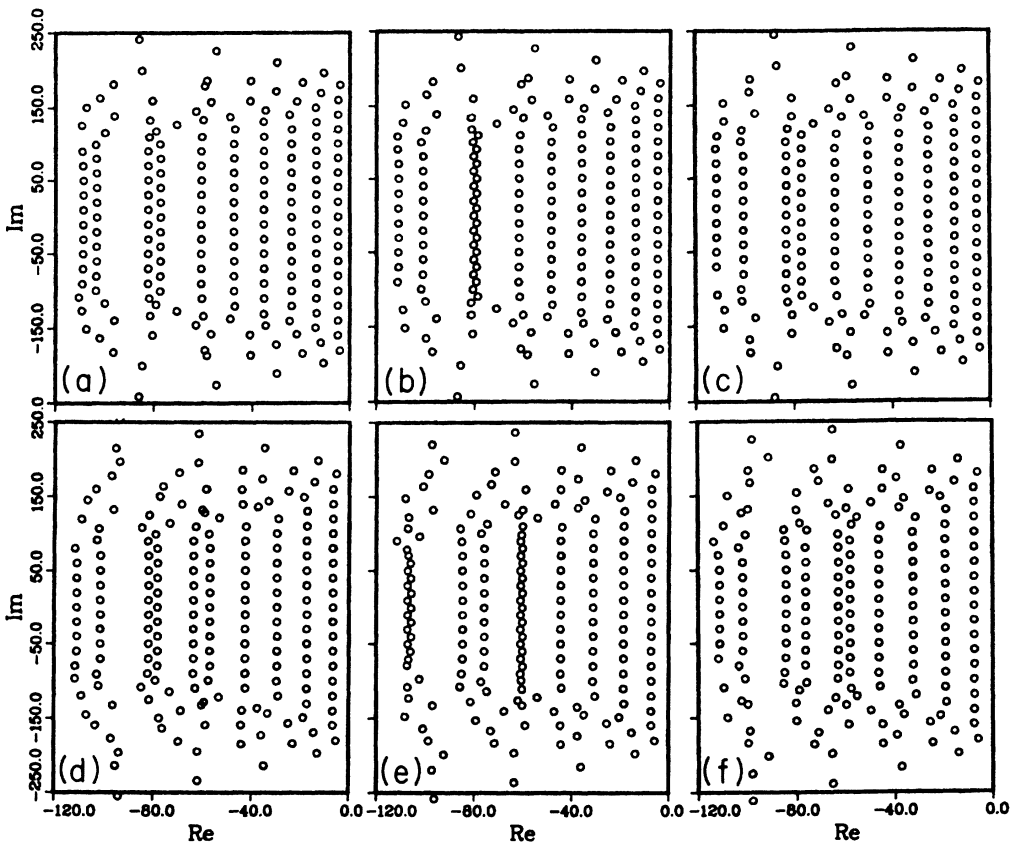

FIG. 3. Local resonance and repulsion of Floquet eigenvalues for case II for $\omega_0=10$. Neighboring lines of eigenvalues move together and repel as ϵ is varied. The resonance occurs along the real axis (the nonlinear part of the spectrum) and moves to lower values of n as ϵ increases. (a) $\epsilon=10.0$, (b) $\epsilon=10.2$, (c) $\epsilon=10.5$, (d) $\epsilon=12.0$, (e) $\epsilon=12.5$, (f) $\epsilon=13.0$.

$$P\left[\theta,t\left|\frac{\pi}{2},0\right.\right]=\sum_{n=1}^{\infty}b_n\left[t,\frac{\pi}{2}\right]\psi_n(\theta)\ . \tag{5.5}$$

If we normalize $\psi_n(\theta)$ on the interval 0 to π, we find $\psi_n(\theta)=\sqrt{2/\pi}\sin(n\theta)$. At time $t=0$,

$$P\left[\theta,0\left|\frac{\pi}{2},0\right.\right]=\delta\left[\theta-\frac{\pi}{2}\right]=\sum_{n=1}^{\infty}b_n\left[0,\frac{\pi}{2}\right]\psi_n(\theta)\ . \tag{5.6}$$

It is easy to show that $b_n(0,\pi/2)=\sqrt{2/\pi}\sin(n\pi/2)$. Let us now substitute Eq. (5.5) into the Fokker-Planck equation (2.6). We obtain

$$\frac{db_m(t,\pi/2)}{dt}=-m^2b_m\left[t,\frac{\pi}{2}\right]+\frac{\epsilon}{2}m\sin(\omega_0t)\times\left[b_{m-1}\left[t,\frac{\pi}{2}\right]-b_{m+1}\left[t,\frac{\pi}{2}\right]\right]\ . \tag{5.7}$$

Thus the coefficients satisfy the same equations as (2.12) and the behavior of the first-passage time for this case is determined by the spectral properties of case IIb.

The average first-passage time may be written

$$\langle t\rangle=\sqrt{2/\pi}\int_0^{\infty}dt\sum_{n=1}^{\infty}\frac{2}{n}b_n\left[t,\frac{\pi}{2}\right]\ . \tag{5.8}$$

We may also express the first-passage time in terms of Floquet states. We first note that

$$b_n\left[t,\frac{\pi}{2}\right]=\sum_{i=1}^{\infty}\sum_{q=-\infty}^{\infty}B_i\left[\frac{\pi}{2}\right]e^{\Lambda_i^{(b)}t}\times\langle n,q|\pi_i^{(b)}\rangle e^{iq\omega_0t}\ . \tag{5.9}$$

If we now combine Eqs. (5.8) and (5.9) and do the time integral in Eq. (5.8), we obtain

$$\langle t\rangle=-\sqrt{2/\pi}\sum_{n=1}^{\infty}\sum_{q=-\infty}^{\infty}B_i\left[\frac{\pi}{2}\right]\frac{\langle n,q|\psi_i^{(b)}\rangle}{(\Lambda_i^{(b)}+iq\omega_0)}\ , \tag{5.10}$$

where

$$\sum_{i=1}^{\infty}B_i\left[\frac{\pi}{2}\right]\langle n|\pi_i^{(b)}(0)\rangle=\begin{cases}\sqrt{2/\pi}\sin\left[\dfrac{n\pi}{2}\right], & \text{for } n \text{ odd}\\ 0, & \text{for } n \text{ even}\ .\end{cases} \tag{5.11}$$

In Figs. 5 and 6 we plot the average first-passage time as a function of external field frequency (Fig. 5) and exter-

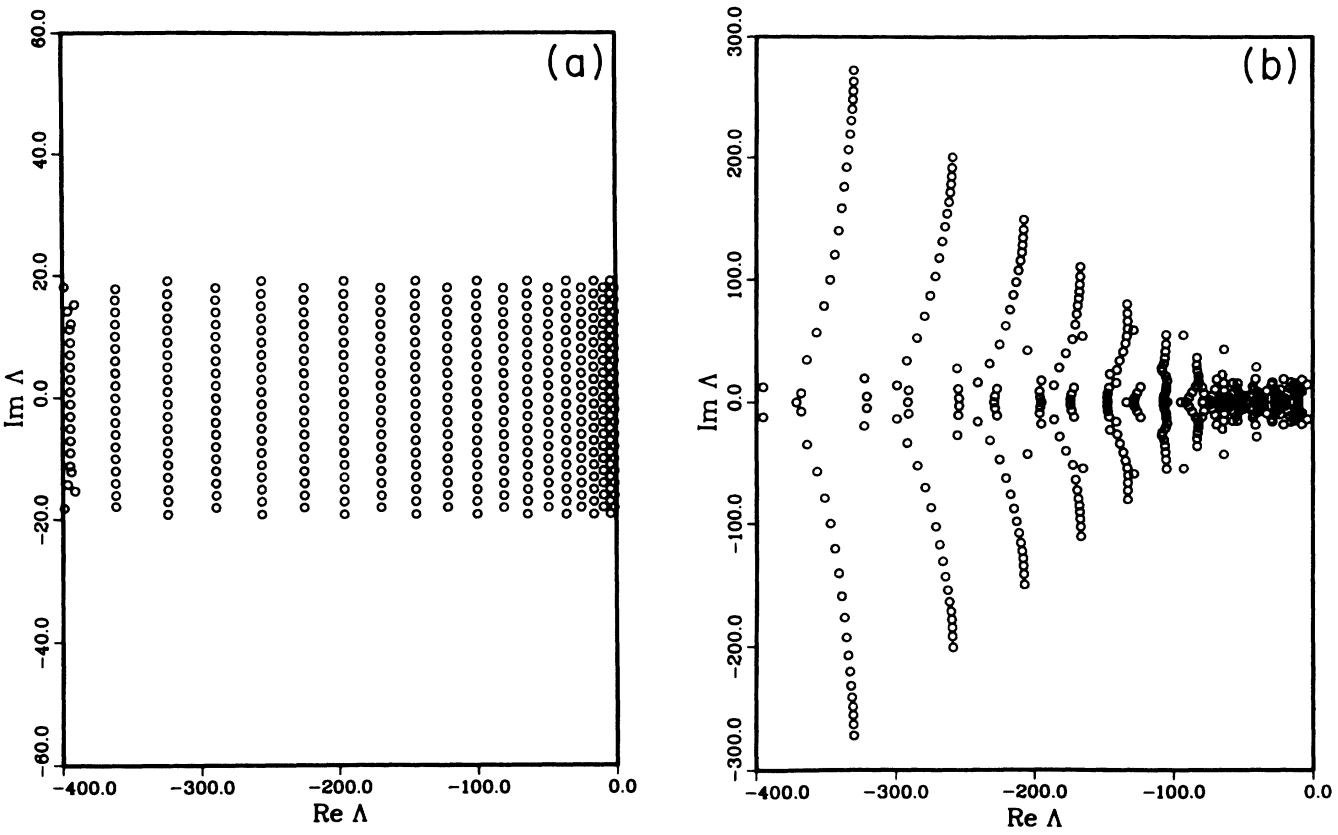

FIG. 4. Floquet spectrum for case IIa for $\omega_0=1.0$ and for the odd submatrix of the cosine block and for a 390×390 matrix. (a) For small external field amplitude ($\epsilon=1.0$) the spectrum exhibits rigid lattice structure. (b) For large external field amplitude ($\epsilon=9.0$), the spectrum exhibits local level repulsion and has an irregular structure.

nal field amplitude (Fig. 6). The numerical results in these figures were obtained by solving Eq. (5.7) numerically for the coefficient $b_n(t,\pi/2)$ for $0<n<100$ and then using these results to perform the integration in Eq. (5.8). The coefficients $b_n(t,\pi/2)$ decay to zero after finite time so that the integral in Eq. (5.8) is easily done. These equations were run until all coefficients $b_n(t,\pi/2)$ $\ll 0.001$.

In Fig. 5, the first-passage time decreases for a finite interval of ω and then increases again. The frequency range in which this decrease occurs coincides with the region in which we observe resonance in the Floquet spectrum (cf. Fig. 3) and appears to be due to resonance between nonlinear rotor modes induced by the stochastic field. Note that the harmonic part of the spectrum (the imaginary part) is not significantly affected by this reso-

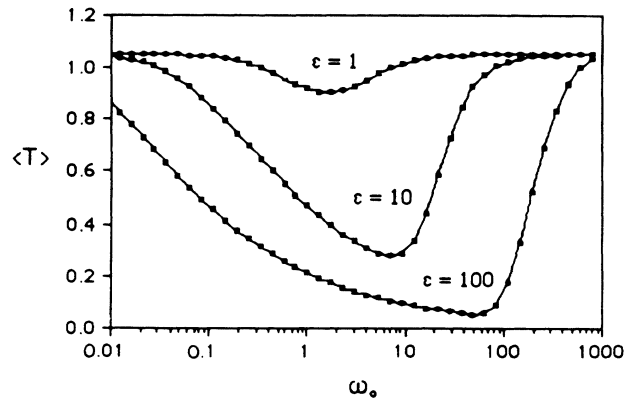

FIG. 5. Plot of mean first-passage time vs ω_0 for $\epsilon_1=\epsilon_2=\epsilon$. Curves for $\epsilon=1.0$, 10.0, and 100.0 are shown. Here $\langle T\rangle=\pi/2\langle t\rangle$, where $\langle t\rangle$ is defined in Eq. (5.8).

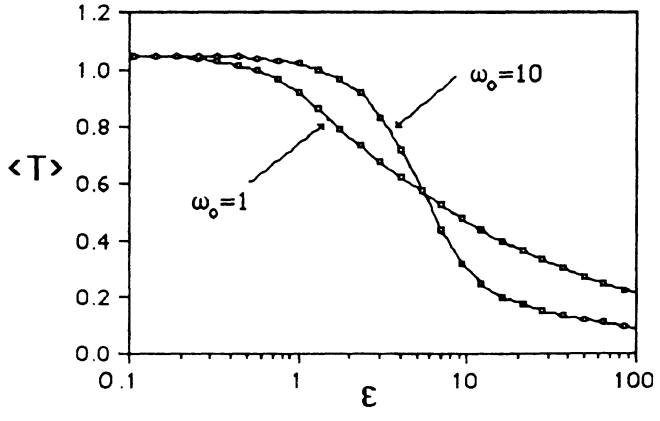

FIG. 6. Plot of mean first-passage time vs ϵ for $\epsilon_1=\epsilon_2=\epsilon$. Curves for $\omega_0=1.0$ and 10.0 are shown. Here $\langle T\rangle=\pi/2\langle t\rangle$, where $\langle t\rangle$ is defined in Eq. (5.8).

nance. A similar resonance in the first-passage time has been observed by Fletcher, Havlin, and Weiss.[10] It is not clear how the resonance observed here is related to the "stochastic resonance" first observed by Benzi, Sutera, and Vulpiani in a double-well model[11] (see also Refs. 12 and 13). However, it is likely that there is a relation. The qualitative behavior of Fig. 5 can be understood as follows. For low frequency and small ϵ the first-passage time is determined primarily by the diffusion process. A simple calculation gives $\langle t \rangle \rightarrow 4/\pi(\pi^3/32)$ for $\epsilon \rightarrow 0$ and $\omega \rightarrow 0$ in agreement with Fig. 5. For high frequency, the field oscillates so rapidly that its effect is averaged out and the first-passage time is again determined primarily by the diffusion process. In between these two limits, resonance effects enhance the first-passage time. The maximum effect appears to occur when $\epsilon \approx \omega$.

Figure 6 shows a drop in the first-passage time as the amplitude ϵ increases. This drop in the first-passage time appears to occur for $\epsilon \leq \omega$ and appears to be related to the shifting of the real parts of the Floquet eigenvalues to larger negative values due to resonance.

VI. SPECTRAL STATISTICS

We have studied the spectral spacing statistics for the Floquet spectrum of the Smoluchowski equation for both cases I and II to determine if the separability of case I and nonseparability of case II is reflected in the statistics of the spacings between eigenvalues in the complex plane.

For a Floquet spectrum which lies on a line, if the eigenvalues are placed randomly on the line, we expect the spacings s between neighboring eigenvalues to satisfy a Poisson distribution $P_{P1}(s)$, where

$$P_{P1}(s)=e^{-s} . \tag{6.1}$$

This has been observed in separable quantum systems of two degrees of freedom which have real eigenvalues.[14] For such quantum systems there are two good quantum numbers (with discrete but infinite range) and the spectrum consists of a superposition of an infinite number of independent pure sequences which therefore appear to be randomly distributed on a line. For a separable system with complex spectrum such as we are considering here, we expect to find a spectral spacing distribution characteristic of a random distribution of points in a plane

$$P_{P2}(s)ds=\frac{\pi}{2}se^{-\pi s^2/4} . \tag{6.2}$$

This is the probability distribution of nearest-neighbor spectral spacings that we expect to observe for the superposition of many independent pure spectral sequences composed of complex numbers.

On the other hand, generic nonseparable systems exhibit spectral repulsion and in the chaotic limit appear to have spectra whose spectral spacing distribution is characteristic of that given by random matrix theory. For systems with real spectra, such as quantum systems whose dynamics is governed by a real symmetric Hamiltonian, resonance and spectral repulsion is associated with a transition to Gaussian-orthogonal-ensemble[15] (GOE)-type spectral statistics. For such systems, the spectral spacing exhibits linear repulsion. On the other hand, the spectral spacing distribution for asymmetric random matrices with Gaussian distribution appear to exhibit cubic repulsion[5] and satisfy a distribution of the form

$$P_{\mathrm{RM}}(s)=As^3e^{-Bs^2} , \tag{6.3}$$

for a two-dimensional random matrix $A=3^4\pi^2 2^{-7}$ and $B=3^2\pi 2^{-4}$.[5] For high-dimension random matrices Grobe, Haake, and Sommers[5] have shown numerically that $P_{\mathrm{RM}}(s)$ is similar to that for two dimensions but lies slightly below the two-dimensional case for small s and above it for large s. Since the dynamics of our Smoluchowski equation is governed by an asymmetric Floquet matrix, we expect that the resonance phenomena we have observed to be accompanied by a transition to random matrix-type behavior characteristic of asymmetric matrices. That is, we expect to see cubic repulsion.

In Figs. 7 and 8, we plot the histograms for the nearest-neighbor spectral spacing for cases I and II, respectively. Figure 7 is the histogram for the lowest 130 points in the spectrum shown in Fig. 2. Figure 8 is the histogram for the lowest 110 points shown in Fig. 4(b). We take only these lowest points in order to attempt to avoid, as much as possible, effects due to the finite size of the matrix. In Fig. 9, we have plotted the integrated spacing distributions $I_{Pi}(s)=\int_0^s ds' P_P(s')$ $(i=1,2)$ and $I_{\mathrm{RM}}(s)=\int_0^s ds' P_{\mathrm{RM}}(s')$ for both Figs. 7 and 8. We unfolded the spectrum by multiplying the level spacings, obtained from the eigenvalue spectrum of the Floquet matrix, by the local average eigenvalue density. From Figs. 7–9, it can be seen that the spectral distribution obeys

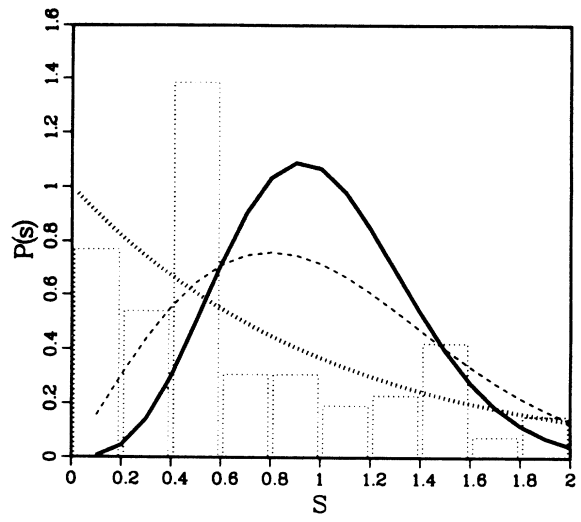

FIG. 7. Histogram of 130 nearest-neighbor spectral spacings for case I for $\omega_0=1.0$, $\epsilon_1=18.0$, and $\epsilon_2=0$. The histogram is close to a Poisson distribution on a line. The hatched line represents a Poisson distribution on a line, the dashed line represents a Poisson distribution in a plane, and the solid represents cubic repulsion characteristic of random matrix theory for asymmetric matrices.

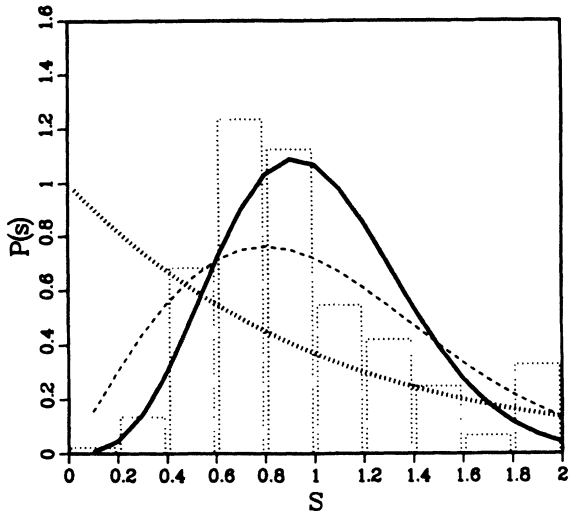

FIG. 8. Histogram of 440 nearest-neighbor spectral spacings for case II for $\omega_0=1.0$ and $\epsilon=9.0$. The histogram is close to a random matrix distribution for cubic level repulsion. The hatched line represents a Poisson distribution on a line, the dashed line represents a Poisson distribution in a plane, and the solid represents cubic repulsion characteristic of random matrix theory for asymmetric matrices.

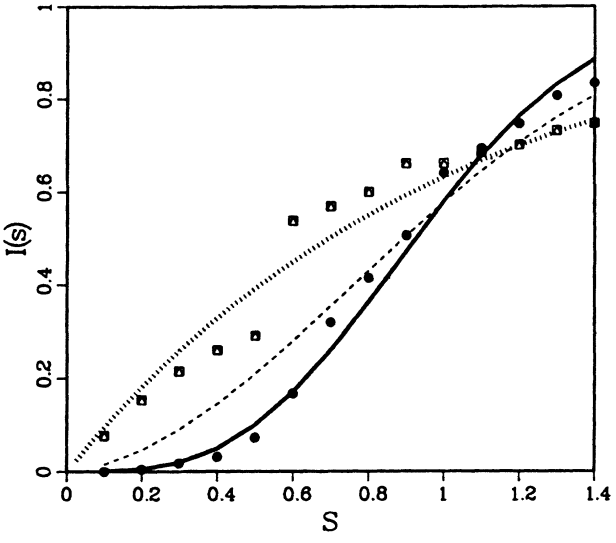

FIG. 9. Integrated spectral spacing distribution for case I and case II. The spectral spacing distribution for case I (squares) is close to that of a Poisson process on a line (hatched line), while the spectral spacing distribution for case II (solid circles) is close to that for cubic level repulsion (solid line). The dashed line refers to a Poisson distribution in a plane. The squares represent the measured spectrum for case I for $\omega_0=1.0$, $\epsilon_1=18.0$, and $\epsilon_2=0$ and the lowest 130 eigenvalues from a 529×529 matrix. The solid circles represent the average spectrum for case II with $\omega_0=1.0$ and $\epsilon=8.5$, 8.75, 9.0, and 9.25. For each value of ϵ 110 eigenvalues from a 390×390 matrix are used to calculate the distribution.

different statistics for these two systems. For the case of single resonance, the spectral spacing statistics follows closely (except for distortions due to rigidity imposed by the harmonic part of the spectrum) a Poisson random process for eigenvalues lying on a line. We did not expect this, but it appears to be due to the fact that the blocks forming the Floquet matrix for case I each have spectra which lie along lines in the complex plane and are not scattered over a two-dimensional region of the complex plane. For case II, on the other hand, the spectral statistics approaches cubic repulsion for small spacings indicating random matrix-type behavior and loss of information about the underlying dynamics governing the stochastic process.

VII. LONG-TIME STATE

Let us denote the eigenstates of the matrix $\langle m,q|\mathcal{W}_{(a)}|n,q'\rangle$ as $|\pi^{(a)}_{(m,q)}(\epsilon)|\rangle$ so that $|\pi^{(a)}_{(m,q)}(\epsilon)\rangle \rightarrow |m,q\rangle$ as $\epsilon\rightarrow 0$. We can expand $|\pi^{(a)}_{(m,q)}(\epsilon)\rangle$ in terms of unperturbed eigenstates

$$|\pi^{(a)}_{(m,q)}(\epsilon)\rangle=\sum_{n=0}^{\infty}\sum_{q=-\infty}^{\infty}|n,q'\rangle\langle n,q'|\pi^{(a)}_{(m,q)}(\epsilon)\rangle\ . \tag{7.1}$$

The probability density of the Brownian rotor in the limit $t\rightarrow\infty$ is determined by the Floquet states whose eigenvalues have zero parts, i.e., $\Lambda^{(a)}_{(0,q)}(\epsilon)=iq\omega_0$. The probability density after a long time can be written

$$P(\theta,t\rightarrow\infty)=\sum_{q=-\infty}^{\infty}\sum_{q'=-\infty}^{\infty}\sum_{n=0}^{\infty}A^{(a)}_{(0,q)}e^{i(q+q')\omega_0 t}\times\langle n,q'|\pi^{(a)}_{(0,q)}\rangle\phi^{e}_{n}(\theta)\ . \tag{7.2}$$

The dependence on ϵ of the components $\langle n,q'|\pi^{(a)}_{(0,0)}\rangle$ of the Floquet eigenstate $|\pi^{(a)}_{(0,0)}\rangle$ is shown in Fig. 10 for $\omega_0=10$. For $\epsilon\leq\omega_0$ a slow spreading occurs in the number of space- and time-dependent Fourier components which contribute to the long-time behavior of the system.

VIII. CONCLUSIONS

We have studied the spectral properties of a driven Brownian rotor in the presence of an angle and time-dependent driving field. In the nonseparable case, the Floquet spectrum shows evidence of nonlinear resonance and spectral repulsion. Evidence of resonance phenomena in highly viscous media has also been observed by other authors. In Refs. 11–13, evidence of resonance like behavior has been observed for a driven Brownian particle in a quartic potential, although none of the authors studied the Floquet spectrum for that case. The effect of resonance on the first-passage time for a particle in a square well has been observed in Ref. 10. The onset of resonance appears to precede the change in the spectral statistics and a loss of "separability" of the corresponding Fokker-Planck equation (we here call a partial differential equation separable if it has a full set of eigen-numbers).

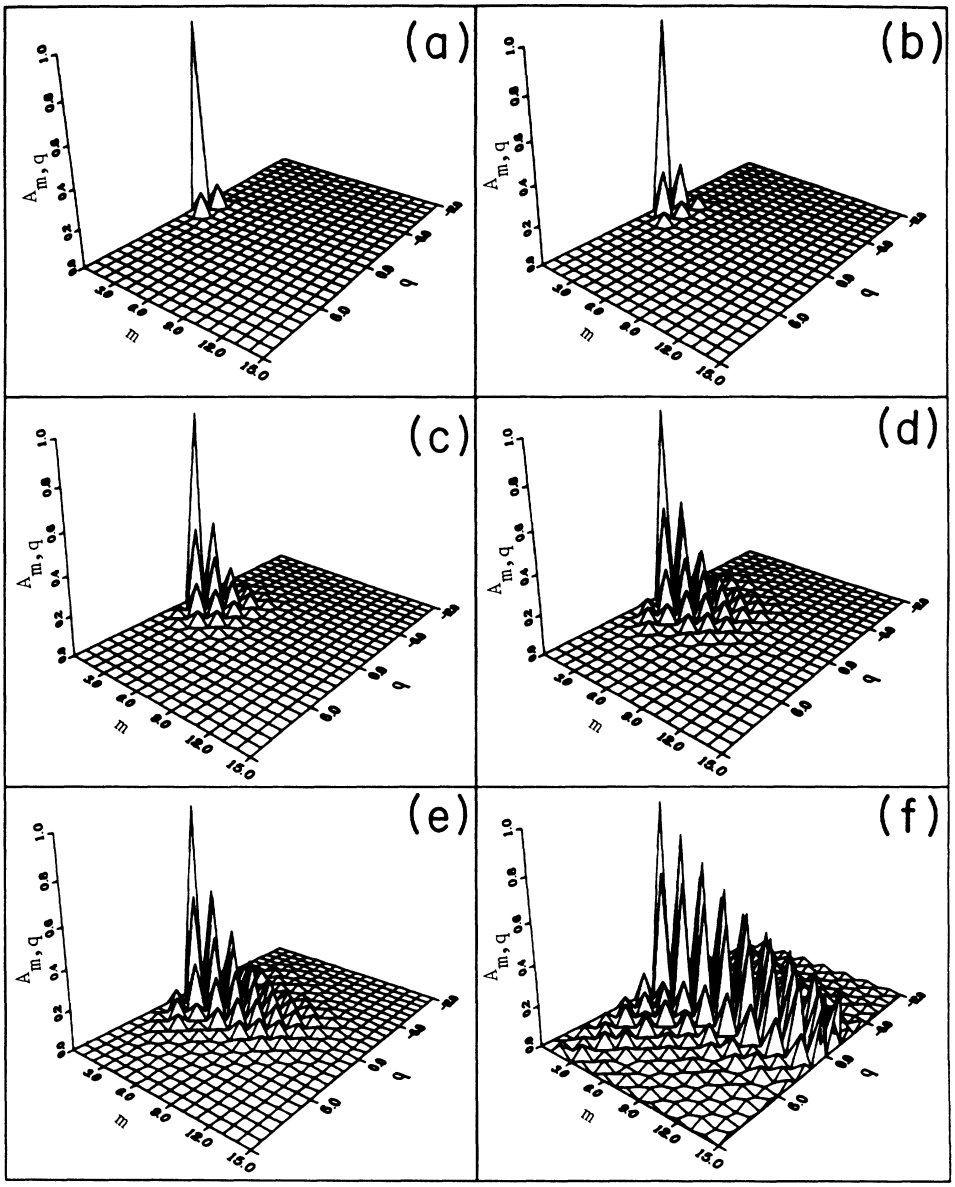

FIG. 10. One of the ground-state eigenvectors for $\omega=10.0$ at different external field strengths. $A_{m,q}$ is the coefficient of the (m,q) component of that eigenvector. (a) $\epsilon=2.5$, (b) $\epsilon=5.0$, (c) $\epsilon=10.0$, (d) $\epsilon=15.0$, (e) $\epsilon=20.0$, (f) $\epsilon=100.0$

ACKNOWLEDGMENTS

The authors wish to thank the Welch Foundation of Texas for partial support of this work (L.E.R. and M.M. under Grant No. F-1051 and Z.-Y.C. under Grant No. F-365). One of us (Z.-Y.C.) would like to thank R. Grobe for useful communications concerning level unfolding and statistics. The computations for this work were performed with a Cray X-MP/24 at the University of Texas System Center for High Performance Computing.

APPENDIX

The matrices $\langle m|\mathcal{V}_{(\alpha)}(t)|n\rangle$ and $\langle m,q|\mathcal{W}_{(\alpha)}|n,q'\rangle$, introduced in Sec. III, are defined in this appendix for the cases $\alpha=a$, b and c.

We first consider $\langle m|\mathcal{V}_{(\alpha)}(t)|n\rangle$. For $\alpha=c$ (case I),

$$\langle m|\mathcal{V}_{(c)}(t)|n\rangle=-m^2\delta_{m,n}-\epsilon\frac{m}{2}(\delta_{n,m-1}e^{-i\omega_0 t}-\delta_{n,m+1}e^{i\omega_0 t}), \tag{A1}$$

with $-\infty\le m$ and $n\le\infty$. For $\alpha=a$ (case IIa),

$$\langle m|\mathcal{V}_{(a)}(t)|n\rangle=-m^2\delta_{m,n}-\epsilon\sin(\omega_0 t)\langle m|V|n\rangle \tag{A2}$$

for $n\ge 1$ and $m\ge 1$, $\langle 0|\mathcal{V}_{(a)}(t)|n\rangle=0$ for $0\le n\le\infty$, and $\langle 1|\mathcal{V}_{(a)}|0\rangle=1/\sqrt{2}$. For $\alpha=b$ (case IIb),

$$\langle m|\mathcal{V}_{(b)}(t)|n\rangle=-m^2\delta_{m,n}-\epsilon\sin(\omega_0 t)\langle m|V|n\rangle \tag{A3}$$

for $n \geq 1$ and $m \geq 1$.

The Floquet matrix $\langle m,q|\mathcal{W}_{(\alpha)}|n,q'\rangle$ can be obtained as follows. For $\alpha=c$ (case I),

$$\langle m,q|\mathcal{W}_{(c)}|n,q'\rangle=(-m^2+iq\omega_0)\delta_{m,n} - \frac{m}{2}[\epsilon_1(\delta_{n,m-1}\delta_{q',q-1} - \delta_{n,m+1}\delta_{q',q+1})] , \quad \text{(A4)}$$

with $-\infty \leq m$ and $n \leq \infty$. For $\alpha=a$ (case IIa),

$$\langle m,q|\mathcal{W}_{(a)}|n,q'\rangle=(-m^2+iq\omega_0)\delta_{n,m}\delta_{q,q'} + \langle m,q|W|n,q'\rangle , \quad \text{(A5)}$$

where $\langle 0,q|W|n,q'\rangle=0$ for $0 \leq n \leq \infty$, $\langle 1,q|W|0,q'\rangle = 1/\sqrt{2}(\delta_{q',q+1}-\delta_{q',q-1})$, and

$$\langle m,q|W|n,q'\rangle = -\frac{m}{4}i(\delta_{n,m+1}-\delta_{n,m-1})(\delta_{q',q+1}-\delta_{q',q-1}) \quad \text{(A6)}$$

for $1 \leq m$ and $n \leq \infty$. For $\alpha=b$ (case IIb),

$$\langle m,q|\mathcal{W}_{(b)}|n,q'\rangle=(-m^2+iq\omega_0)\delta_{n,m}\delta_{q,q'} + \langle m,q|W|n,q'\rangle , \quad \text{(A7)}$$

for $1 \leq m$ and $n \leq \infty$.

[1] T. H. Seligman, J. J. M. Verbaarschot, and M. R. Zirnbauer, Phys. Rev. Lett. **53**, 215 (1984).

[2] T. Terasaka and T. Matsushita, Phys. Rev. A **32**, 538 (1985).

[3] W. A. Lin and L. E. Reichl, Phys. Rev. A **36**, 5099 (1987); **37**, 3972 (1988).

[4] W. A. Lin and L. E. Reichl, Phys. Rev. A **40**, 1055 (1989).

[5] R. Grobe, F. Haake, and H.-J. Sommers, Phys. Rev. Lett. **61**, 1899 (1988).

[6] H. Risken, *The Fokker-Planck Equation* (Springer-Verlag, Berlin, 1984).

[7] D. Escande, Phys. Scr. **T2/1**, 126 (1982).

[8] J. H. Shirley, Phys. Rev. B **138**, 979 (1965).

[9] L. E. Reichl, J. Stat. Phys. **53**, 41 (1988).

[10] J. E. Fletcher, S. Havlin, and G. H. Weiss, J. Stat. Phys. **51**, 215 (1988).

[11] R. Benzi, A. Sutera, and A. Vulpiani, J. Phys. A **14**, L453 (1981); **18**, 2239 (1985).

[12] B. McNamara, K. Wiesenfeld, and R. Roy, Phys. Rev. Lett. **60**, 2626 (1988).

[13] P. Jung and P. Hanggi, Europhys. Lett. **8**, 505 (1989).

[14] G. Casati, B. V. Chirikov, and I. Guarneri, Phys. Rev. Lett. **54**, 1350 (1985).

[15] T. A. Brody, J. Flores, J. B. French, P. A. Mello, A. Pandey, and S. S. M. Wong, Rev. Mod. Phys. **53**, 386 (1981).